contacts are depicted in Figure 2. The average Ag···Ag distance is 3.34 (14) Å, which is significantly shorter than the one observed in the cubane-like isomer of $(Ph_3P)_4Ag_4I_4$ (3.483 Å)[10] but longer than the respective distance in $(Ag_2I_3)_n^{n-}$ (3.045 Å).[11]

The $Et_3Te^+$ ion is normal; the Te–C distances and C–Te–C angles are all as expected.[2] There are four Te···I contacts, the shortest being 3.822 (6) Å (with I(4)) and the longest being 4.231 (6) Å (with I(5)). All these interactions are approximately linear with the Te–C bonds, as postulated for such interactions to be the secondary bond interactions.[12]

**Acknowledgment.** We are thankful to the University of Manitoba Research Grants Committee for the financial support of this work and to Prof. John E. Drake, Chairman, Department of Chemistry and Biochemistry, University of Windsor, for allowing the time to use the Syntex $P2_1$ diffractomer.

**Registry No.** $Et_3TeI$, 104746-44-3; $Ag[S_2P(OEt)_2]$, 1186-32-9; $Et_3TeAg_4I_5$, 113273-48-6; $Et_2Te$, 627-54-3; $EtSP(S)(OEt)_2$, 2524-09-6.

**Supplementary Material Available:** Tables of I···I distances, I···I···I, I···Te–C, Ag···Ag···Ag, and I–Ag···Ag angles, and anisotropic thermal parameters, an ORTEP plot of $(Ag_4I_5)_n^{n-}$ showing all the symmetry-related positions, and a figure displaying the contents of the unit cell (5 pages); a table of observed and calculated structure factors (12 pages). Ordering information is given on any current masthead page.

(10) Teo, B. K.; Calabrese, J. C. *J. Am. Chem. Soc.* **1975**, *97*, 1236.
(11) Kildea, J. D.; White, A. H. *Inorg. Chem.* **1984**, *23*, 3825.
(12) Alcock, N. W. *Adv. Inorg. Chem. Radiochem.* **1972**, *15*, 1.

Contribution from the Department of Chemistry, Carnegie Mellon University, Pittsburgh, Pennsylvania 15213

## Spin-Density Distributions in *meso*-Alkyl/Aryl Hybrid Porphyrin Cation Radicals

Michael Atamian, Richard W. Wagner, Jonathan S. Lindsey,* and David F. Bocian*

*Received October 20, 1987*

Porphyrin cation radicals have been identified as intermediates in the catalytic cycles of a number of heme-containing peroxidases and catalases.[1-6] Cation radicals of pigments that are related to porphyrins also play an essential role in photosynthesis.[7-12] Consequently, considerable effort has been focused on the characterization of these oxidized systems. Ring oxidation of a metalloporphyrin yields either a $^2A_{2u}$ or a $^2A_{1u}$ ground state; the specific ground state is determined by the nature of the ring substitutents and/or the axial ligands to the metal ion.[13-16] Molecular orbital calculations indicate that the unpaired charge density in a $^2A_{2u}$ cation resides primarily on the pyrrole nitrogen and *meso*-carbon atoms whereas this density in a $^2A_{1u}$ cation resides primarily on the pyrrole $\alpha$- and $\beta$-carbon atoms.[17,18] The resulting spin-density distributions in the two types of cations have been probed in detail by Fajer and co-workers who examined a number of $\beta$- and meso-substituted porphyrin cation radicals via electron paramagnetic resonance (EPR) techniques.[16-18] These studies allowed the characterization of subtle variations in spin density as a function of the nature of the substituent group.

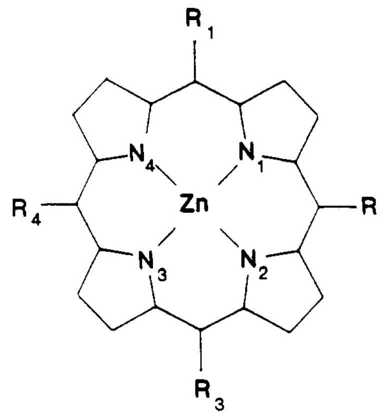


| | $(CH_2)_4CH_3$ | p-$(CH_3O_2C)$-Φ |
|---|---|---|
| 1: | $R_1$, $R_2$, $R_3$, $R_4$ | — |
| 2: | $R_1$, $R_2$, $R_3$ | $R_4$ |
| 3a: | $R_1$, $R_2$ | $R_3$, $R_4$ |
| 3b: | $R_1$, $R_3$ | $R_2$, $R_4$ |
| 4: | $R_1$ | $R_2$, $R_3$, $R_4$ |
| 5: | — | $R_1$, $R_2$, $R_3$, $R_4$ |

**Figure 1.** Atomic labeling scheme for the *meso*-alkyl/arylporphyrins.

Previous EPR studies have primarily focused on porphyrin cations whose substituents are symmetrically disposed about the meso- or $\beta$-positions of the ring.[14,17,19,20] The limitation of these studies to symmetrical systems is in large part due to the difficulty of preparing in good yield and high purity porphyrins that are asymmetrically substituted at the periphery of the macrocycle. Recently, one of our groups has developed a methodology which allows ready access to porphyrins that are asymmetrically meso-substituted (hybrid porphyrins).[21,22] The basic synthetic strategy can also be used to enhance the efficiency of preparation of other exotic meso-substituted porphyrins such as isotopically labeled species. The availability of these various systems affords the opportunity to probe more systematically and in greater detail

(1) Gans, P.; Marchon, J.-C.; Reed, C. A.; Regnard, J. R. *Nouv. J. Chim.* **1981**, *5*, 203.
(2) Phillipi, M. A.; Shimonura, E. T.; Goff, H. M. *Inorg. Chem.* **1981**, *20*, 1322.
(3) Dunford, H. B.; Stillman, J. S. *Coord. Chem. Rev.* **1976**, *19*, 187.
(4) Hewson, W. D.; Hager, L. P. In *The Porphyrins*; Dolphin, D., Ed., Academic: New York, 1979; Volume 7, p 295.
(5) Schulz, C. E.; Rutter, R.; Sage, J. T.; Debrunner, P. G.; Hager, L. P. *Biochemistry* **1984**, *23*, 4743.
(6) Dunford, H. B.; Araiso, T.; Job, D.; Ricard, J.; Rutter, R.; Hager, L. P.; Wever, R.; Kast, W. M.; Boelens, R.; Ellfolk, N.; Ronnberg, M. In *The Biological Chemistry of Iron*; Dunford, H. B., Dolphin, D., Raymond, K. N., Sieker, L., Eds.; D. Reidel: Dordrecht, The Netherlands 1982, pp 337–355.
(7) Norris, J. R.; Katz, J. J. In *Photosynthetic Bacteria*; Clayton, R. K., Sistrom, W. R., Eds.; Plenum: New York, 1978, pp 397–418.
(8) Norris, J. R.; Uphaus, R. A.; Crespi, H. L.; Katz, J. J. *Proc. Natl. Acad. Sci. U.S.A.* **1971**, *68*, 625.
(9) Lubitz, W.; Lendzian, F.; Scheer, H.; Gottstein, J.; Plato, M.; Mobius, K. *Proc. Natl. Acad. Sci. U.S.A.* **1984**, *81*, 1401.
(10) Lubitz, W.; Isaacson, R. A.; Abresch, E. C.; Feher, G. *Proc. Natl. Acad. Sci. U.S.A.* **1984**, *81*, 7992.
(11) Lubitz, W.; Lendzian, F.; Scheer, H. *J. Am. Chem. Soc.* **1985**, *107*, 3341.
(12) Horning, T. L.; Fujita, E.; Fajer, J. *J. Am. Chem. Soc.* **1986**, *108*, 323.
(13) Dolphin, D.; Forman, A.; Borg, D. C.; Fajer, J.; Felton, R. H. *Proc. Natl. Acad. Sci. U.S.A.* **1971**, *68*, 614.
(14) Fajer, J.; Borg, D. C.; Forman, A.; Felton, R. H.; Vegh, L.; Dolphin, D. *Ann. N. Y. Acad. Sci.* **1973**, *206*, 349.
(15) Felton, R. H.; Owen, G. S.; Dolphin, D.; Forman, A.; Borg, D. C.; Fajer, J. *Ann. N. Y. Acad. Sci.* **1973**, *206*, 504.
(16) Fajer, J.; Davis, M. S. In *The Porphyrins*; Dolphin, D., Ed.; Academic: New York, 1979; Vol. 4, pp 197–256.
(17) Fajer, J.; Borg, D. C.; Forman, A.; Adler, A. D.; Varedi, V. *J. Am. Chem. Soc.* **1974**, *96*, 1238.
(18) Fajer, J.; Borg, D. C.; Forman, A.; Dolphin, D.; Felton, R. H.; *J. Am. Chem. Soc.* **1970**, *92*, 3451.
(19) Glazkov, Yu. V.; Kuzovkov, P. V.; Shul'ga, A. M. *Zh. Prikl. Spektrosk.* **1973**, *18*, 320.
(20) Glazkov, Yu. V.; Kuzovkov, P. V.; Shul'ga, A. M. *Zh. Prikl. Spektrosk.* **1973**, *19*, 305.
(21) Lindsey, J. S.; Hsu, H. C.; Schreiman, I. C. *Tetrahedron Lett.* **1986**, *27*, 4969.
(22) Lindsey, J. S.; Schreiman, I. C.; Hsu, H. C.; Kearney, P. C.; Marguerettaz, A. M. *J. Org. Chem.* **1987**, *52*, 827.

0020-1669/88/1327-1510$01.50/0 

**Table I.** Hyperfine Splittings and $E_{1/2}$ Values for the Porphyrin Cation Radicals

| zinc porphyrin[a] | $E_{1/2}$,[b] V | hyperfine splitting, G (MHz)[c] | |
|---|---|---|---|
| **1** | 0.68 | $^{14}N_{1,2,3,4}$ | 1.66 (4.64) |
| **2** | 0.75 | $^{14}N_{1,2}$ | 1.66 (4.64) |
| | | $^{14}N_{3,4}$ | 1.60 (4.48) |
| **3a** | 0.81 | $^{14}N_{1}$ | 1.66 (4.64) |
| | | $^{14}N_{3}$ | 1.45 (4.07) |
| | | $^{14}N_{2,4}$ | 1.57 (4.39) |
| **3b** | 0.81 | $^{14}N_{1,2,3,4}$ | 1.60 (4.48) |
| **4** | 0.87 | $^{14}N_{1,4}$ | 1.64 (4.60) |
| | | $^{14}N_{2,3}$ | 1.50 (4.20) |
| **5** | 0.92 | $^{14}N_{1,2,3,4}$ | 1.42 (3.98) |
| **6** | 0.84 | $^{14}N_{1,2,3,4}$ | 1.41 (3.95) |
| | | $^{13}C_{meso}$ | 5.72 (16.02) |
| | | $^{1}H_{o\text{-phenyl}}$ | 0.24 (0.67) |

[a] See Figure 1 for structures. [b] V versus Ag/AgCl in $CH_2Cl_2$, ~0.1 M TBAP. [c] Uncertainties in the hyperfine splittings: $^{14}N$, ± 0.01 G (~0.03 MHz); $^{13}C$, ±0.02 G (~0.06 MHz). Other simulation parameters: hyperfine splittings, $^{1}H_{o\text{-aryl}}$ = 0.34 G (0.96 MHz), $^{1}H_{\alpha\text{-pentyl}}$ = 2.75 G (7.70 MHz); Gaussian fwhm = 0.49 G (1.37 MHz).

the structural and electronic properties of the porphyrin moiety.

In this note, we report EPR and electrochemical data for the cation radicals of the six possible structural permutations of a porphyrin that contains *meso*-pentyl and/or *meso*-*p*-(methoxycarbonyl)phenyl substituents. These species, the structures of which are shown in Figure 1, present one example of the diverse types of substituted porphyrins that are readily available with our new synthetic strategy. In addition, we report the EPR spectrum of the ZnTPP-*meso*-$^{13}C_4$ (TPP = 5,10,15,20-tetraphenylporphyrin) cation radical and thereby directly probe the spin density at the *meso*-carbon atoms of the porphyrin ring.

## Experimental Section

The details of the synthesis and characterization of the hybrid porphyrins will be reported separately. TPP-*meso*-$^{13}C_4$ was prepared from pyrrole (Aldrich) and benzaldehyde-$\alpha$-$^{13}C$ (MSD Isotopes, 99.99% isotopic purity) via the basic synthetic strategy that has been previously reported by Lindsey et al.[21,22] Zinc was inserted into the porphyrins according to standard procedures.[23] The cation radicals of the zinc porphyrins were generated electrochemically in a nitrogen-atmosphere glovebox (Vacuum Atmospheres). The oxidations were performed in standard three-compartment cells with platinum working and counter electrodes and a Ag/AgCl reference. Cyclic voltammograms and bulk electrolyses were accomplished by using a Princeton Applied Research (PAR) Model 175 universal programmer in conjunction with a PAR Model 173 potentiostat. In all cases $CH_2Cl_2$ (Fisher reagent grade, distilled from $P_2O_5$ in vacuo) was used as the solvent and tetrabutylammonium perchlorate, TBAP (Kodak, recrystallized twice from absolute ethanol and dried at 111 °C in vacuo), was used as the supporting electrolyte (~0.1 M). The integrities of the oxidized species were monitored by cyclic voltammetry, coulometry, and optical absorption spectroscopy.

X-band EPR spectra were recorded at room temperature on an IBM Instruments ER300 spectrometer. The concentrations of the samples ranged from 0.2 to 0.5 mM. The microwave power and magnetic field modulation amplitude were typically 20 mW and 0.7 G, respectively.

## Results and Discussion

The X-band EPR spectra of the six porphyrin cation radicals are shown in Figure 2. The hyperfine splittings for the $^{14}N$, $^{1}H_{\alpha\text{-pentyl}}$, and $^{1}H_{o\text{-aryl}}$ nuclei are summarized in Table I. These hyperfine splittings were obtained via computer simulation of the EPR spectra. The simulated and observed spectra are essentially superimposable. The uncertainty in the $^{14}N$ hyperfine splittings listed in Table I is ±0.01 G (~0.03 MHz). All of the oxidized species are $^{2}A_{2u}$ cations as is evidenced by the relatively large $^{14}N$ hyperfine splittings. The splittings for the four equivalent $^{14}N$ nuclei in the two parent porphyrins **1** and **5** range from 1.66 to 1.42 G, respectively. The difference in the $^{14}N$ hyperfine splittings

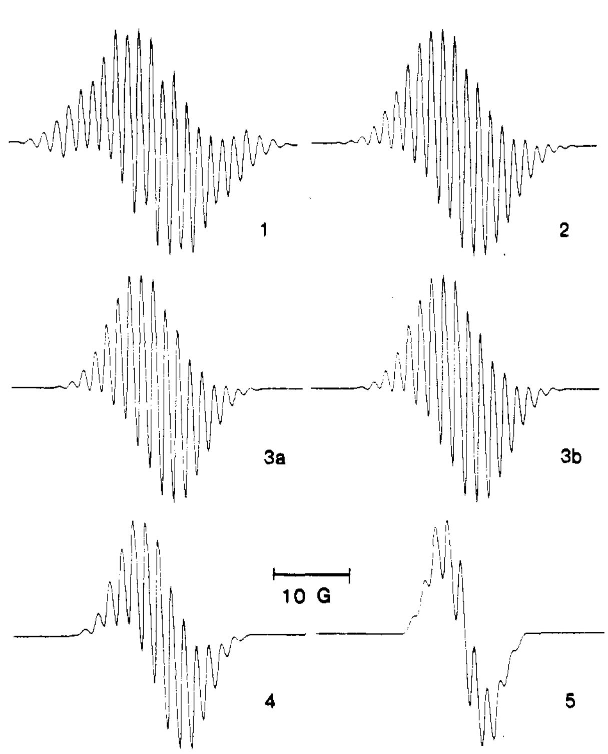


**Figure 2.** Room-temperature, X-band EPR spectra of the *meso*-alkyl/arylporphyrin cations **1**–**5**.

between the *meso*-tetraalkyl- and *meso*-tetraarylporphyrin cations reflects a difference in spin density of ~0.007 at each nitrogen atom.[16] For cations of the pentyl/*p*-(methoxycarbonyl)phenyl hybrids, the equivalence of the $^{14}N$ nuclei is removed and the magnitudes of the hyperfine splittings of the various inequivalent nitrogen atoms lie between those that are observed for the two parent porphyrin cations. The various $^{1}H_{\alpha\text{-pentyl}}$ and $^{1}H_{o\text{-aryl}}$ nuclei are also inequivalent in the binary hybrids; however, the resulting inequivalence in the spin density at these positions is negligible because the protons are removed by one or more carbon atoms from the porphyrin $\pi$ system. Consequently, the hyperfine splittings for the $^{1}H_{\alpha\text{-pentyl}}$ and $^{1}H_{o\text{-aryl}}$ nuclei of all of the binary hybrids were taken to be the same as those for the two parent porphyrins, 2.75 and 0.34 G, respectively.

Comparison of the $^{14}N$ hyperfine splittings for the hybrid porphyrin cation radicals provides insight into the influence of structural asymmetry on the spin density distribution. The *trans*-dialkyldiarylporphyrin **3b** contains four magnetically equivalent $^{14}N$ because each lies between two *meso*-carbon atoms that bear different substituents. The $^{14}N$ hyperfine splitting for these equivalent nuclei is 1.60 G. This value is closer to the hyperfine splitting for the tetraalkylporphyrin cation **1** than for the tetraaryl species **5**. This result indicates that the influence of the pentyl substituents on the spin density at the pyrrole nitrogen atoms outweighs that of the aryl groups. This disparate influence on the spin density is also manifested in the $^{14}N$ hyperfine splittings of the two different tri/monosubstituted compounds **2** and **4**. Both of these hybrids contain two sets of two equivalent $^{14}N$ nuclei. Each hybrid contains one set in which a nitrogen atom is straddled by both a *meso*-pentyl and *meso*-aryl group. This substitution pattern is the same as that experienced by each nitrogen atom in **3b**. The hyperfine splitting for this type of nitrogen atom in **2** is the same as that of **3b** (1.60 G) whereas this splitting in **4** is larger (1.64 G). The other equivalent sets of nitrogen atoms in **2** and **4** are straddled by *meso*-carbon atoms that bear identical substituents. The $^{14}N$ hyperfine splittings for the sets that are flanked by either pentyl or aryl groups are 1.66 or 1.50 G, respectively. These values are skewed in the direction of those observed for **1**. This skewedness is also reflected in the hyperfine splittings of the *cis*-dialkyldiaryl hybrid **3a**, which contains all three of the types of magnetically distinct $^{14}N$ nuclei that are found in the other hybrids.

(23) Fuhrhop, J.-H.; Smith, K. M. In *Porphyrins and Metalloporphyrins*; Smith, K. M., Ed.; Elsevier: Amsterdam, 1975, p 798.

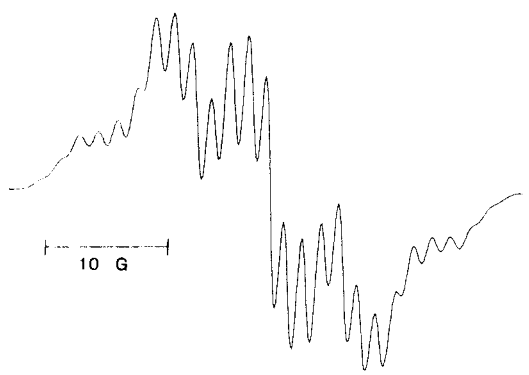


**Figure 3.** Room temperature, X-band EPR spectrum of the ZnTPP-*meso*-$^{13}C_4$ cation **6**.

Although the pentyl substituent has a greater influence on the spin density distribution than does the aryl group, this disparity is not manifested in the half-wave potentials ($E_{1/2}$) for the six different meso-substituted porphyrins. These potentials are summarized in Table I. As can be seen, the $E_{1/2}$ values of **3a** and **3b** are equal and approximately midway between those of **1** and **5**. In addition, the replacement of each pentyl group by an aryl group results in an approximately linear shift of the $E_{1/2}$ to a more anodic potential (~60 mV/group). It seems reasonable that this disparity in the behavior of the redox potentials versus the $^{14}N$ hyperfine splittings is due to the fact that the $E_{1/2}$ is a property of the entire macrocycle whereas the hyperfine splittings reflect the electronic properties at specific sites on the ring.

In view of the asymmetry in the $^{14}N$ hyperfine splittings of the binary hybrid porphyrin cations, it would be of interest to examine the spin density on the *meso*-carbon atoms. The spin density at this position is calculated to be considerably greater than at the pyrrole nitrogen atoms. To our knowledge, however, $^{13}C$ hyperfine splittings have not been previously reported even for a symmetrically substituted porphyrin cation. As a consequence, we examined the EPR spectrum of the ZnTPP-*meso*-$^{13}C_4$ cation radical **6**. This EPR spectrum is shown in Figure 3, and the hyperfine splittings that were obtained via computer simulation of the spectrum are given in Table I. The $^{13}C$ hyperfine splitting is 5.72 ± 0.02 G (~0.06 MHz). This value can be compared with that which is estimated from the modified McConnell relation[24]

$$a_i = 30.5\rho_i - 13.9\sum_j \rho_j$$

where $a_i$ is the hyperfine splitting in gauss and $\rho_i$ and $\rho_j$ are the spin densities at the *meso*- and $\alpha$-carbon atoms, respectively. The values of $\rho_i$ and $\rho_j$, which are calculated with (without) configuration interaction, are 0.193 (0.158) and −0.0094 (0.0066).[18] These calculated spin densities result in a predicted *meso*-$^{13}C$ hyperfine splitting of 6.15 G (4.64 G), which is in reasonable agreement with the experimentally observed splitting.

**Acknowledgment.** We thank Anne Marguerettaz for preparing ZnTPP-*meso*-$^{13}C_4$. This work was supported by Grants GM-36238 (J.S.L.) and GM-36243 (D.F.B.) from the National Institute of General Medical Sciences.

**Registry No.** **1**, 106469-09-4; **1**$^+$, 113451-71-1; **2**, 113451-68-6; **2**$^+$, 113451-72-2; **3a**, 113451-76-6; **3a**$^+$, 113451-75-5; **3b**, 113451-69-7; **3b**$^+$, 113451-73-3; **4**, 113451-70-0; **4**$^+$, 113451-74-4; **5**, 64466-25-7; **5**$^+$, 113474-61-6.

(24) Karplus, M.; Fraenkel, G. K. *J. Chem. Phys.* **1961**, *35*, 1312.

# Additions and Corrections

1987, Volume 26

**Steven G. Rosenfield, Hilde P. Berends, Lucio Gelmini, Douglas W. Stephan, and Pradip K. Mascharak***: New Octahedral Thiolato Complexes of Divalent Nickel: Syntheses, Structures, and Properties of $(Et_4N)[Ni(SC_5H_4N)_3]$ and $(Ph_4P)[Ni(SC_4H_3N_2)_3]\cdot CH_3CN$.

Page 2793. In Table I, the values of *a* and *c* for compound **3** are interchanged; the correct values are $a$ = 15.090 (4) Å and $c$ = 18.958 (5) Å.—Pradip K. Mascharak